Aqueous sample holders for high-frequency electron spin resonance

Jeff P. Barnes and Jack H. Freed[a)]
Baker Laboratory of Chemistry, Cornell University, Ithaca, New York 14853-1301

(Received 7 February 1997; accepted for publication 1 April 1997)

A quasioptical approach is utilized to design a resonator and sample holder for aqueous samples for high-frequency (250 GHz) electron spin resonance (ESR) spectroscopy. A disk shaped sample geometry was chosen to match the field contours of the fundamental mode in a Fabry–Perot resonator. A transmission-line analysis is used to determine the optimum sample geometry while taking into account diffractive effects of the sample and the sample holder on the far infrared (FIR) radiation field. FIR-ESR spectra of several aqueous solutions of nitroxide spin labels, including membrane vesicles and a labeled protein, are shown to demonstrate the success of the technique. © *1997 American Institute of Physics.* [S0034-6748(97)01007-1]

I. INTRODUCTION

Electron spin resonance (ESR) spectroscopy of nitroxide labeled biopolymers has proven itself to be an important method in elucidating the slower macromolecular motions of proteins[1] as well as the faster, internal dynamics of proteins[2] and DNA,[3] the dynamics and ordering of phospholipid membranes,[4] and protein–protein, protein–DNA, and protein–lipid interactions.[5] The intrinsically high sensitivity of ESR allows one to work with just nanomoles of labeled compounds, which is especially useful for making nondestructive measurements for biopolymers in their native state, such as membrane associated proteins[6] or even measurements in living cells. Since almost all systems of biological interest consist of either biopolymers dissolved in aqueous solutions or involve phospholipid membranes whose interactions with the surrounding aqueous medium strongly influence their structure and dynamics, the ability to record ESR spectra of aqueous samples is vital.

The development of high-frequency ESR techniques holds several advantages for the study of nitroxide-labeled biopolymers. For the study of dynamics, high-frequency ESR extends the range over which spectral line shapes are sensitive to the molecular motions of nitroxides. For 250 GHz ESR, a sensitivity to reorientational correlation times as short as 1 ps is possible.[7] High-frequency ESR of spin labeled biopolymers is expected to be an important technique for linking the structure of biopolymers to their dynamics and function, for example in the study of some of the internal motions of nucleic acids in DNA (0.02–4 ns)[8] and vibrational motions that involve the domain structures of proteins (1–20 ps).[9] High-frequency ESR also has enhanced g-tensor resolution for nitroxides, which allows their use as a sensitive probe of the polarity of their local environment.[10] The higher intrinsic sensitivity of high-frequency ESR suggests applications toward samples where volume size or spin-probe concentration is limited, as is the case for many systems of biological interest.

To date, applications of ESR above 35 GHz to aqueous biological systems have been limited because of dielectric absorption. Studies involving aqueous solutions of vesicles have recently been carried out at 95 GHz using 0.15 mm i.d. quartz capillaries placed inside a cylindrical TE_{01n} cavity.[11] Studies of spin-labeled proteins at 140 GHz also utilized a microwave cavity and a quartz capillary sample holder, but have employed only lyophylized, frozen, or partly humidified samples.[12] However, the removal of water from biological systems severely perturbs their structure, dynamics, and biological functions, so it would be advantageous to develop a technique to record high-frequency ESR spectra of aqueous samples.

The design of sample holders for high frequency ESR is greatly aided by a knowledge of the complex dielectric constant, $\epsilon=\epsilon'+i\epsilon''$, of liquid water in the far infrared (FIR) range. Extensive measurements of ϵ below 40 GHz have been tabulated.[13] More recent measurements cover the frequency range from 1 to 13 500 GHz.[14–16] The data show that both ϵ' and ϵ'' generally decrease with increasing frequency above 20 GHz, until resonant absorption bands due to intermolecular librations (as opposed to relaxation processes) begin to occur at around 10 THz.[13] The value of $\epsilon=5.5-i6.0$ at 250 GHz used in this work represents an average of the interpolated values from the cited references.

Given that ϵ is generally decreasing above 20 GHz, it would seem that by working at higher frequencies, dielectric losses can be reduced. However, an aqueous sample is still a very lossy sample for ESR spectroscopy in the FIR region. Our own experience at 250 GHz has demonstrated that one must carefully keep even submicroliter volumes of an aqueous sample from contact with an E field antinode in a resonator, or else the resonator becomes too lossy to be able to conveniently obtain ESR spectra. Thus there are two trends to consider for increasing frequency. First, λ is decreasing, so the overall thickness of an aqueous sample must also decrease to be able to keep the sample out of the E field. Second, ϵ'' is also decreasing, which allows one to increase the ratio of the sample thickness to λ for higher frequencies. To conveniently consider these effects, one introduces the attenuation constant, $\alpha=(2\pi/\lambda)\mathrm{Im}(\sqrt{\epsilon})$.[17] It enters into a simple transmission line analysis in a Beer's law form, i.e., the resonator field amplitudes decay as $e^{-\alpha d}$, where d is the aqueous sample thickness. The expression for α clearly shows how it increases by decreasing λ, ignoring for the moment the variation of ϵ with λ. One finds from measure-

[a)]Electronic mail: jhf@msc.cornell.edu

 0034-6748/97/68(7)/2838/9/$10.00

ments of α on liquid water in the FIR region that the decreasing value of ϵ'' with decreasing λ does not fully offset the effect of the $1/\lambda$ term in α. Thus α increases with increasing frequency. For example, at room temperature, $\epsilon = 62 - i30$ and $\alpha = 0.36\ \mathrm{mm}^{-1}$ at 9.3 GHz, while at 173 GHz, $\epsilon = 7.3 - i8.5$ and $\alpha = 5.1\ \mathrm{mm}^{-1}$, and at 250 GHz, $\epsilon = 5.5 - i6.0$ and $\alpha = 6.0\ \mathrm{mm}^{-1}$. These values emphasize the importance of using thinner samples at higher frequencies. The transmission line analysis used below implicitly includes α and the aqueous sample thickness, d, and thus takes into account the dielectric losses in an aqueous sample as discussed above. It will allow us to determine an optimum value of d for sensitivity to ESR for any given value of ϵ, or equivalently, α.

Fortunately we find that, for the optimum sample geometry, high-frequency (250 GHz) ESR spectra can be obtained on submicroliter volumes with a sensitivity adequate for studies of many aqueous samples of biological interest. In this article we describe a sample holder which allows one to obtain 250 GHz ESR spectra of aqueous samples with volumes from 0.1 to 1 μL. For the spectrometer operating in a transmission mode, we demonstrate a spectral sensitivity for an optimum sample geometry of 2×10^9 spins/G, with higher sensitivites expected for a reflection-mode spectrometer.[18,19]

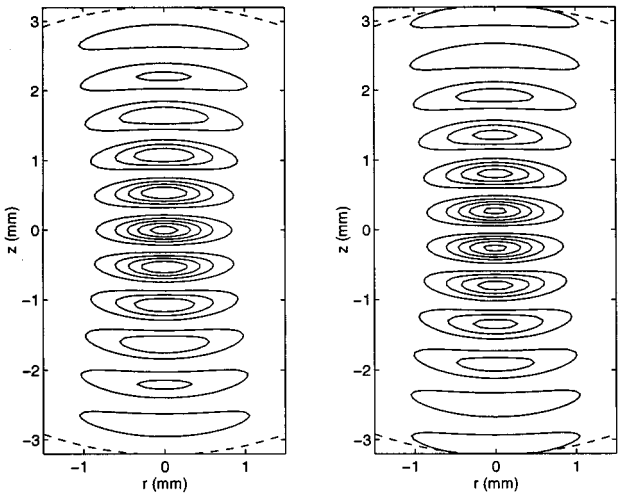

FIG. 1. A contour plot of $|E|^2$ (left) and $|H|^2$ (right) for a cross section of a fundamental Hermite–Gaussian mode with $\lambda = 1.2$ mm in a FP resonator. The mirrors (dashed lines) have radii of curvature of 4.0 mm, which is lower than that used for the 250 GHz ESR spectrometer in order to more clearly demonstrate diffractive effects. The contours are at 10%, 30%, 50%, 70%, and 90% of maximum intensity. Features to be noted are the higher field intensities near the beam waist at $z = 0$, and the finite curvature of the field nodes away from the beam waist.

II. DESIGN AND EXPERIMENTS

The quasioptical techniques that have been utilized to construct and successfully operate ESR spectrometers at 170 and 250 GHz at Cornell have been discussed in detail elsewhere.[18–20] These designs use a Fabry–Perot (FP) resonator consisting of either two spherical mirrors (confocal) or of one flat and one spherical mirror (semiconfocal) to enhance sensitivity. Descriptions of the eigenmodes of FP resonators in terms of ''Gaussian beam modes'' have been given.[20,21] For ESR, the FP resonators are designed to operate in the lowest order, or fundamental, beam mode, because higher order modes are broader in radial extent and thus suffer from lower field intensities and greater power losses from out of the sides of the open FP resonator. It is the fundamental mode of an FP resonator that we shall discuss in detail.

For the fundamental beam mode, the E and H fields are both nearly normal to the direction of propagation, are nearly linearly polarized, and the field intensities are cylindrically symmetric about the axis of propogation. This mode resembles a plane wave in which the field amplitudes have a Gaussian profile normal to the direction of propagation. Figure 1 is a contour plot of $|E|^2$ and $|H|^2$ for a cross section of the linearly polarized fundamental mode in a confocal FP resonator, using dimensions typical for an ESR experiment. The $|H|^2$ maxima fall in between those of $|E|^2$. Note that the mode is broader in radial extent at the two spherical mirrors of the cavity than in the middle, where the fields have greatest intensity. At this region of the mode, called the beam waist, the field nodes are planar surfaces; nearer to the spherical mirrors the nodes of the fields assume a more spherical shape. These considerations suggest that using a flat layer of water as the sample holder geometry, placed near the beam waist of the mode, offers two advantages: the power density of the H field, and hence sensitivity to ESR, is greatest here, and it is easier to fabricate a flat sample holder than a curved one.

For the special case of the fundamental mode, the beam waist radius, ω_0, can be defined as the radial distance from the beam axis to the point at which the field amplitude has fallen to e^{-1} of its maximum value. It can be calculated from the radii of curvature of the two mirrors and the mirror-to-mirror separation.[22] Sensitivity to ESR absorption will rapidly drop off for samples with a radial dimension of $> 2\omega_0$, so this represents a reasonable compromise between limited sample volumes and ESR sensitivity. For the 250 GHz ESR spectrometer at Cornell, $\omega_0 \approx 2.2$ mm.

For the flat sample holder geometry, there is an advantage to using the confocal resonator instead of the semiconfocal resonator. For the semiconfocal resonator, the beam waist occurs at the surface of the flat mirror, where there also must exist an E field node. Attempting to place a flat sample as close to the flat mirror as possible gives one only half the sample volume to work with as compared to the confocal case. In addition, covering the coupling iris of a mirror with a dielectric layer has been found to prevent efficient coupling into the resonator.[23]

In order to determine the interaction of the radiation field with this sample holder, we utilized the transmission line analysis as outlined earlier. First, since our sample holder must be thinner than a wavelength, we may assume the extent of the sample holder along the beam axis is such that the phase front of the radiation field within the sample holder remains flat. That is, we model the beam mode within the

sample holder as a plane wave at normal incidence upon a series of flat plates, each of a given thickness, dielectric constant $\epsilon=\epsilon'+i\epsilon''$, and magnetic susceptibility $\chi=\chi'+i\chi''$. The FP resonator is modeled as a waveguide with an impedance of free space, and the mirrors are represented by complex shunt impedances. Solving this one-dimensional ''transmission-line'' problem is more tractable than solving for the three-dimensional E and H fields in the sample/resonator system,[24] especially when the sample and sample holder consist of several layers of different dielectric materials.

There are some features of the fundamental Hermite–Gaussian mode that are neglected when it is modeled as a plane wave: the ''phase slip'' of the plane wave with respect to the beam mode, the growth of the radial extent of the beam mode within the sample holder, and effects such as a shift in the beam waist, and thus the phase of the beam, upon reflection from a dielectric surface.[25] We will quantify the error introduced by the first two approximations. We can introduce the phase slip into the analysis to first order by replacing the wave number in each dielectric, $2\pi/(\lambda/n)$, with $2\pi/(\lambda/n)-(\lambda/n)/\pi\omega_0^2$, where $n=\mathrm{Re}\sqrt{\epsilon}$ is the index of refraction of the dielectric at 250 GHz. This was found to reduce the computed sensitivities by $\approx$5%–20%, for which the greatest depressions occurred for those sample holder geometries which were least sensitive to ESR. However, this did not significantly alter the derivation of the optimum sample holder geometry. A measure of the error involved in the neglect of the beam radius growth within the sample holder is to compute the power that emerges from a plate of thickness d and index of refraction n with the same beam waist radius, ω_0, as the beam had when it entered the far side of the plate. Power that emerges with a beam radius greater than ω_0 is assumed to be lost from the open resonator. The computation is similar to that of the beam growth within a FP diplexer,[26] so we only repeat the result here:

$$P=\frac{4}{r}(1-r^2)\sum_{k=1,3,5,\ldots}\frac{r^k}{3+a^2k^2+\dfrac{1+4a^2k^2}{1+a^2k^2}}, \tag{1}$$

where $r=(n-1)/(n+1)$ is the internal reflection coefficient and $a=d\lambda/n\pi\omega_0^2$ is a measure of the divergence of the beam within the plate. We require that $d\ll 1$ mm for $\lambda=1.2$ mm. The assumption of $d=0.5$ mm, $\omega_0=2.0$ mm, and $1.5\leqslant n\leqslant 3.0$ yields power losses of only 29 dB down from the incident beam, a negligible amount.

The transmission-line analysis yields the amplitudes of the E and H fields in the resonator and in each layer of the sample holder by requiring the continuity of the tangential components of the fields at the surfaces between the dielectrics, and determining the propagation constant within each layer from the values of ϵ and χ. It has been observed that the polarization of the fields in the 250 GHz ESR spectrometer in the transmission mode remain esentially fixed, so this is assumed in the analysis. The resulting system of linear equations were solved to yield the complex reflection, R, and transmission, T, coefficients for the resonator/sample holder system.

The analysis of ESR sensitivity depends upon the method of detection.[27] For our experiments, the 250 GHz ESR spectrometer was setup in a transmission mode, and the detector was a biased InSb bolometer. ESR absorption is detected as a periodic change in the transmitted power through the resonator as the static magnetic field is modulated. Thus we have

$$\text{ESR sensitivity}\propto\left.\frac{\partial|T|^2}{\partial\chi''}\right|_{\chi=0}. \tag{2}$$

We mention three other aspects of this model for clarity. The first is that, as the beam propagates from the sample holder to the mirror, it picks up an anomalous phase shift due to diffractive effects. This will influence the mirror-to-mirror separations for which the resonator is calculated to be in resonance, which in turn alters the beam waist radius and therefore the filling factor (proportional to ω_0^{-2}) of the system. However, the effect is a small one as long as the resonator is operated within the ''stable'' region.[22] For example, for a confocal resonator with 25.4 mm radius-of-curvature mirrors, an increase in the mirror separation from 6 to 12 mm increases the beam waist radius from 1.78 to 2.04 mm. For our experiments the mirror separation was kept as close to 8 mm as possible and the effect of the beam waist on the sensitivity was ignored. Also, there is an initial large diffractive loss in iris coupled open resonators that occurs because the radiation field from a small iris expands rapidly, and some power coupled into the resonator is lost out its sides.[28] Since the value of the shunt impedance of the irises, Y models the Q of the resonator, it takes into account some of these diffractive losses in the resonator/sample holder system, and so we must treat Y as an unknown. For a mesh or beamsplitter coupled resonator which does not suffer from these initial losses, the value of Y could be determined *a priori* from the measured Q and maximum transmission of the empty resonator.[18,29]

One must have the ability to vary the mirror separation in order to tune for resonance, and to independently alter the height from the sample to the bottom mirror in order to place an aqueous sample at an E-field node. Figure 2 shows a design that allows this. We have found that the temperature of this arrangement can be controlled from $+80$ to -196 °C to an accuracy of ± 0.5 °C using flowing dry N_2 gas. For these very thin samples, we have also found that the Helmholtz coils used for field modulation can be replaced with a solenoid to increase modulation amplitude and decrease coupling to the superconducting magnet Dewar.

In order to tune the resonator containing an aqueous sample for maximum transmission, it was experimentally found that one had to go through several cycles of separately varying the distance from the bottom mirror to the sample, x, and from the sample to the top mirror, y. The reason for this can be seen in Fig. 3, which is a plot of the computed power transmitted through a resonator with a 0.02-mm-thick water layer inside as a function of (x,y). The result of the transmission-line analysis is periodic in both x and y with period equal to $\lambda/2=0.6$ mm, because the spread of the beam within the FP resonator is ignored. However, the model correctly shows that the presence of the aqueous layer

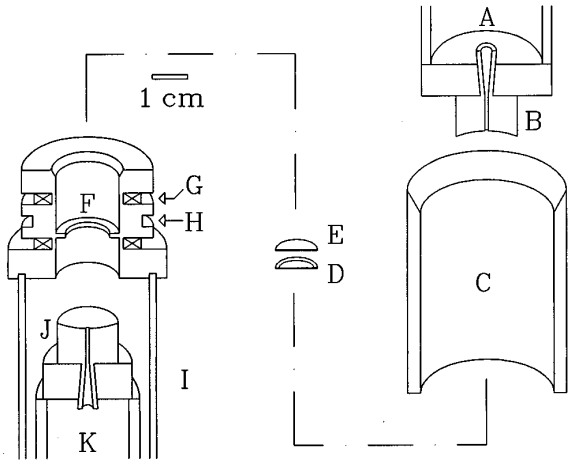

FIG. 2. Schematic for the modulation coil and the etched quartz plate sample holder. (A) Top optiguide which guides the FIR beam toward the detector. (B) Top mirror of the FP resonator shown with its coupling iris and scalar feed horn. (C) Sleeve to help align the optical components. The aqueous sample holder consists of (D) the bottom quartz plate with an etched circular depression and (E) the top quartz plate. It sits in the center of the modulation coil form, (F), on a ridge whose surface was machined so as to keep the sample normal to the optical axis of the resonator. The coilform includes grooves for (G) Helmholtz modulation coils and (H) N_2 gas for temperature control. (I) A support by which the modulation coil and sample holder are raised independently of the mirrors of the FP resonator. (J) The bottom mirror of the resonator. (K) The bottom optiguide, pointing to the FIR source.

in the FP resonator implies that both x and y must be varied to reach a transmission maximum. Thus any device designed to automatically keep a resonator containing an aqueous sample on resonance would need to simultaneously adjust both of these dimensions.

Shown in Fig. 4 is the recorded transmission through the FP resonator when loaded with a 0.017-mm-thick aqueous sample, as the height of the sample holder was varied while the resonator length remained fixed. The transmission is nearly periodic with a period of 0.6 mm, but there are two transmission peaks every half-wavelength, one prominent

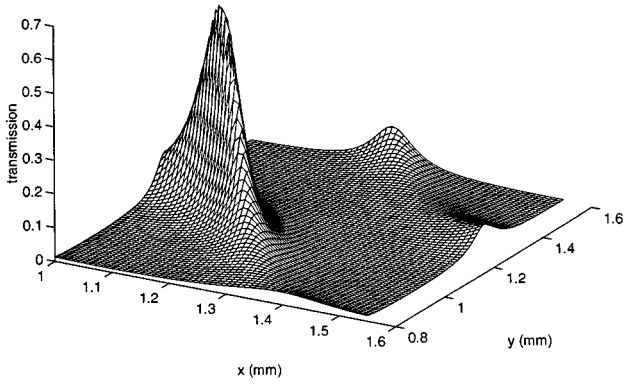

FIG. 3. A plot of the transmitted power through a FP resonator with a 0.02-mm-thick aqueous layer present, calculated using the transmission line analysis with mirror impedances of $0.2+i4.0$. The distance from the bottom mirror to the water layer is x, and from the water layer to the top mirror is y.

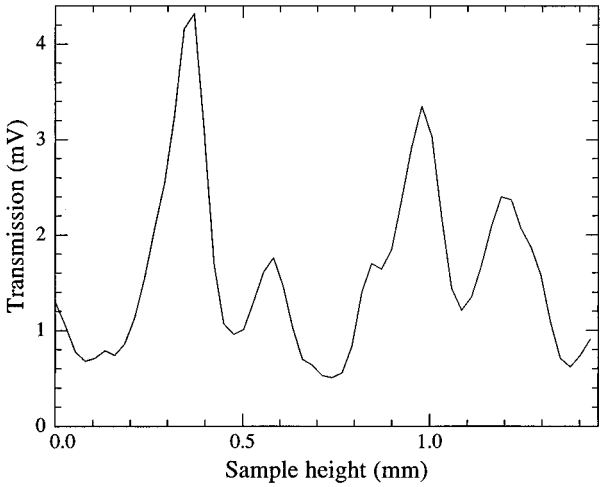

FIG. 4. Experimentally observed transmission through the FP resonator when a 0.017-mm-thick water layer in a quartz sample holder is present. As the height of the sample holder is varied, the resonator goes through periodic transmission maxima when the water layer is positioned within an E-field node.

and one less so, and the prominent transmission peaks are found to decrease slightly as the aqueous sample is moved away from being nearly equidistant between the two mirrors. The less prominent peaks are probably due to higher order radial modes of the resonator that are excited when all the optical components are not perfectly aligned. The maximum transmission peak corresponds to placing the sample nearest to the beam waist. To summarize, the ESR spectrometer with a thin aqueous sample present in the FP resonator is tuned for maximum transmission by placing the sample at the beam waist, and both resonator length and sample height must be varied to accomplish this.

The sample holder was constructed from fused quartz coverslips which are polished optically flat, are 12 mm in diameter and 0.165 mm thick.[30] Quartz has a measured index of refraction of $n=2.13$ and an attenuation constant of $\alpha=0.0006$ dB/mm in the FIR region.[21] Other materials that could be used include polymers such as poly-(4-methylpentene-1) (TPX), polyethylene terephthalate (PETE), high-density polyethylene (HDPE), or polystyrene. These polymers have low enough loss tangents for FIR to be useful,[31] although they are easily deformed when very thin. Another possibility is an etched silicon wafer. However, we have experimentally found that borosilicate glasses were too lossy to be useful as samples holders, at least at 250 GHz.

A cylindrically symmetric, flat depression with a radius of 10 mm was created in a coverslip by dissolving the quartz (SiO_2) with a 48% hydrofluoric acid solution at room temperature. Paraffin was used to mask a ring of 1 mm width at the edge of the plate.[32] This was done to ensure that when two plates were pressed together to form an enclosed space between them, they would rest flat against one another. The etching rate was found to be 32 μm/h, so the thickness of the aqueous samples was accurately known. The etching creates sloped sides with a width of 0.7 mm for the deepest plates, but these sides are far beyond the beam waist radius and should cause few scattering losses. The etched bottoms of

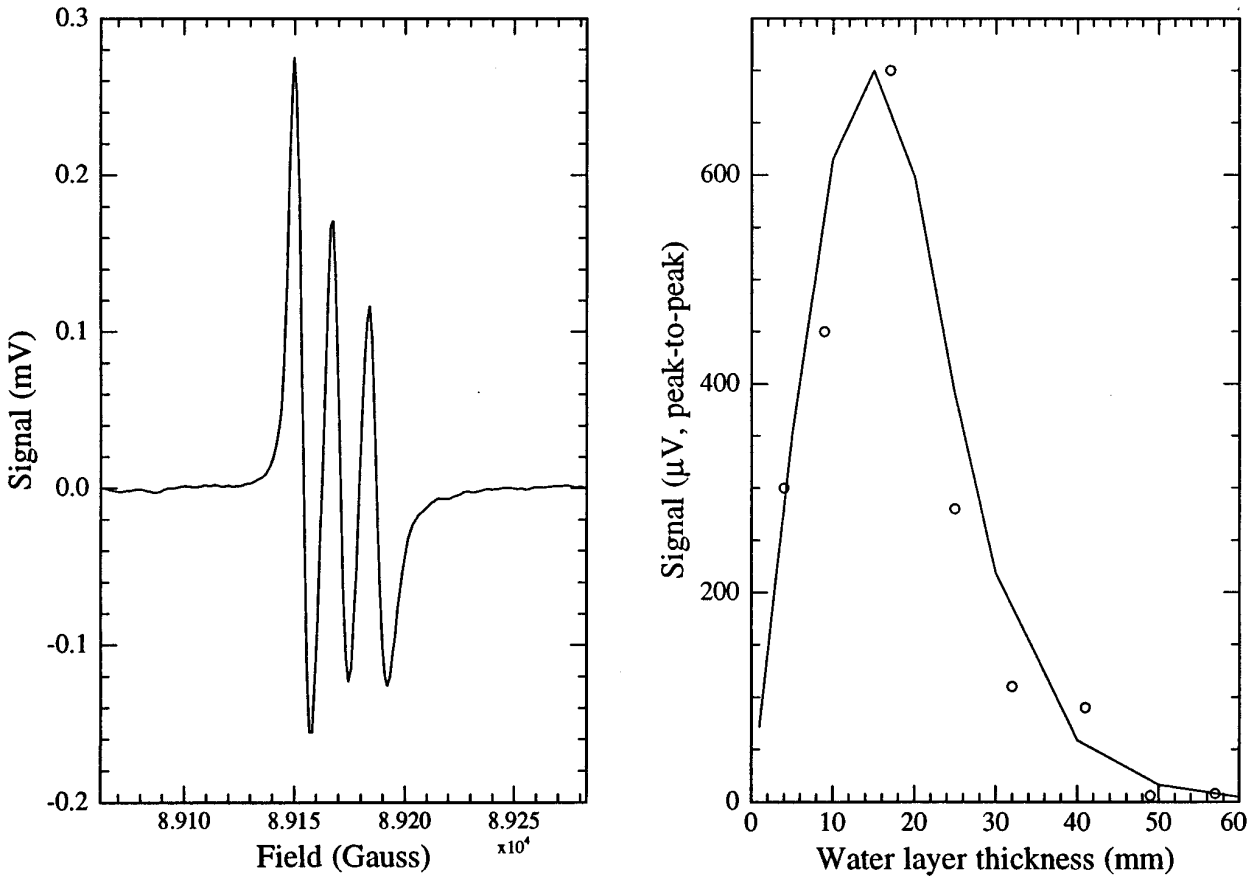

FIG. 5. (Left) 250 GHz ESR spectrum of a 0.27 mM tempamine aqueous solution at 15 °C. The water layer was 0.009 mm thick, with 0.14 μL held in the ESR active region of the FP resonator between two quartz plates 0.165 mm thick. The signal-to-noise ratio for the spectrum is 750. The small molecule tumbles nearly isotropically with a rotational correlation time of 30 ps. (Right) A plot of the peak-to-peak signal voltage detected for aqueous samples of various thicknesses. The curve is from the transmission line analysis as described in the text.

the quartz plates are smooth, with a few pits of micron size that can be observed under a microscope.

To produce a sample, an aqueous solution is placed in the etched depression and a second quartz plate is carefully placed over the top so no air bubbles are trapped in the sample. If necessary, a thin layer of grease can be applied along the flat outer rim of the plate to seal the sample and prevent evaporation. Two etched plates can be used to form thicker aqueous samples. The thickness of the aqueous samples used in this study ranged from 4 to 60 μm, and from 1 to 10 μL of fluid was used to fill them, but the ESR-active volumes of the samples ranged from only 0.1 to 1 μL.

An aqueous solution of 0.27 mM tempamine (4-amino-2,2,6,6-tetramethyl-piperidine-*N*-oxyl) was used as a standard sample. The sample was not deoxygenated before use, although this could be accomplished even for delicate biological samples by using a sample holder constructed from TPX.[33] The presence of O_2 in air saturated water adds a homogeneous linewidth of $\leqslant$0.15G for nitroxides.[34] In general, this added linewidth is small in comparison to the contribution from the partly averaged anisotropic g tensor for high-frequency ESR on nitroxides: note that the linewidth of the 250 GHz ESR spectrum of 0.27 mM tempamine, molecular weight 171, in an aqueous solution at 15 °C has a 7G peak-to-peak linewidth (Fig. 5, left). For the purpose of analyzing high-frequency ESR line shapes to determine motional and ordering parameters, this additional linewidth can usually be neglected.

The sample holder sat in the resonator so that the thicker quartz plate was facing the detector. The resonator was tuned for maximum transmission, and FIR-ESR spectra were recorded at 15 °C. The static magnetic field modulation coil was driven with 100 V peak-to-peak sine wave at 80 kHz, which is less than 1G of modulation amplitude. The signal was detected with an InSb bolometer operated at 4 K, passed to a low-noise preamp with a gain of 200, and into a phase sensitive detector with a postdetection bandwidth of 0.312 Hz. A typical 250 GHz ESR spectrum is shown in Fig. 5 (left). The results for the various aqueous sample thicknesses are recorded in Table I. The higher noise level observed for the thinnest sample seems to be due to microphonics. The vibration of the modulation coils modulates the transmitted power of the resonator, and this noise increases as the transmission of the resonator increases.

Figure 5, right, also shows a plot of the signal intensity as a function of the aqueous sample thickness. The line represents the sensitivity as computed from the transmission line analysis using the following parameters: $n=2.13$ and a

loss tangent of tan $\delta=\epsilon''/\epsilon'=0.0006$ for the quartz plates in the FIR, and $n=2.60$ with tan $\delta=1.1$ for the aqueous sample, and $Y=0+i30$ for the shunt impedance of the mirrors. The sensitivities were determined for each sample geometry by first varying the sample height and resonator length to find the maximum calculated transmission, which mimics what is experimentally done; the sensitivity is then computed using those dimensions. The value of Y was chosen to give a good fit by eye, but does not come from a least-squares fit, since for sensitivity measurements, we expect random perturbations to always decrease the measured response from some maximum value, i.e., the errors are not distributed normally.

Figure 6 is a plot of the calculated sensitivity of a sample holder consisting of two plates of equal thickness, d, and an aqueous layer of thickness t, and using a fixed mirror impedance of $Y=0+i30$. The results for utilizing quartz and HDPE as the plate material are shown. As d increases, absorption of the FIR radiation in the plate lowers the sensitivity, but a curious increase can also be observed at larger values of d for the quartz sample holder. The dip in sensitivity at $d=0.14$ mm occurs as the optical path length through the sample holder approaches a half-wavelength. In order to keep the aqueous layer at an E field node, the sample holder is positioned in the resonator so that the outer surfaces of the quartz plates experience E field antinodes. Since tangential E and H fields are continuous across a dielectric boundary, a larger E field penetrates the sample holder, resulting in higher dielectric losses and the reflection of most of the incident power back toward the source. This last effect can be alleviated by lowering the Q of the resonator which requires changing the iris size in the mirrors or using a mesh-coupled resonator. Figure 7 shows how the calculated sensitivity changes for a few quartz plate sample holder dimensions as the imaginary part of the shunt impedance, b, is changed. Increasing b means a smaller coupling iris in the mirrors and thus a higher resonator Q, but dielectric losses also increase so there exists an optimum value of b. Best sensitivity for the $d=0.14$-mm-thick quartz plate sample holder is achieved at lower resonator Q than for the $d=0.04$ mm sample holder in order to offset the increased dielectric losses. However, overall maximum sensitivity is still best achieved by using thinner quartz plates.

This finding seemed counterintuitive, because at $d=0.14$ mm the sample holder acts like a low-Q dielectric resonator, increasing $|H|^2$ at the aqueous layer by a factor of

TABLE I. Sensitivity of 250 GHz ESR to an aqueous solution of 0.27 mM tempamine as a function of the sample thickness. The aqueous samples were held in a flat quartz-plate sample holder and all spectra were obtained at 15 °C.

Thickness (μm)	% transmission	Signal (μV)	Noise (μV)	Signal/noise
4	45	300	1.6	190
9	40	450	0.6	750
17	60	700	0.7	990
25	23	280	0.3	930
32	10	110	0.4	280
40	9	90	0.6	150
48	3	6	0.3	20
57	2	8	0.2	40

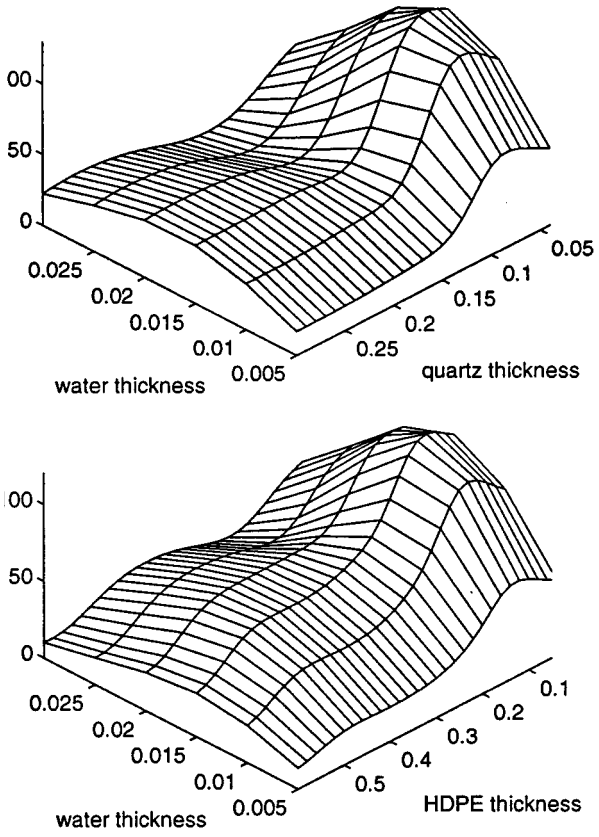

FIG. 6. A plot of the sensitivity of (top) the quartz and (bottom) the HDPE plate sample holder in a transmission-mode spectrometer as a function of the thickness of the water layer and of both plates (units of mm), and assuming a fixed iris impedance.

≈ 4 over the fields within the FP resonator. The ability of a dielectric to increase sensitivity to ESR by increasing $|H|^2$ at the sample is a well known effect which has been observed at lower frequencies.[35] It seems that sample placement to maximize transmission conflicts with the ability to minimize dielectric losses. Interestingly, the transmission-line analysis shows that the effect is *reversed* when a reflection mode spectrometer is utilized instead of a transmission mode. (Sensitivity for the reflection mode resonator is defined as the derivative of the reflected power with respect to χ'' of the aqueous sample.) This is seen by comparison of Fig. 6 with Fig. 8, which plots the sensitivity for a quartz plate sample holder with a 0.02-mm-thick aqueous sample layer, in a reflection mode resonator. Peaks in the sensitivity for the reflection mode occur approximately where dips occur for the transmission resonator. Compared to the transmission mode setup, in a reflection mode spectrometer (1) the spectrometer is no longer symmetric along its optical axis about the aqueous layer, and (2) the field amplitudes in the resonator are a maximum when the power delievered to the detector is a minimum. As a result, the maximum sensitivity to ESR occurs when the resonator is tuned slightly off resonance.[27] Interestingly, for cases where the loaded resonator is very lossy, the computed ESR sensitivity shows a third maximum for when the resonator is tuned directly on resonance. In general, however, gains in sensitivity are expected for a reflection mode spectrometer versus the transmission mode

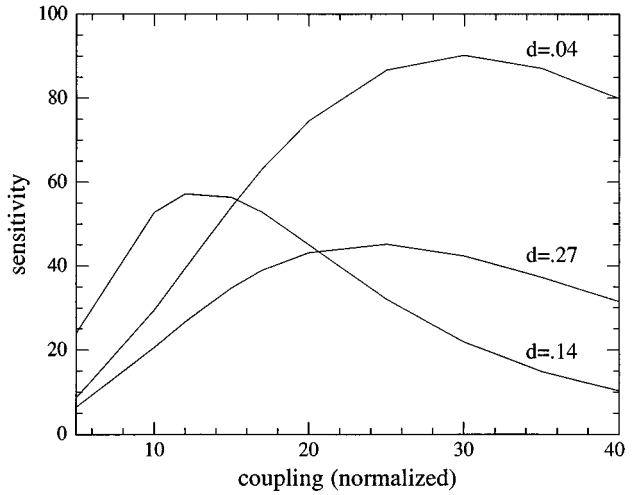

FIG. 7. The calculated sensitivity of three flat quartz plate sample holders as a function of the shunt impedance of the mirrors, normalized to the impedance of free space. The aqueous sample thickness is 0.025 mm, and the quartz plates are 0.040, 0.140, and 0.270 mm thick. The range of b represents a range of resonator Q due to coupling of from ≈ 5 to 400 with the lower Q for smaller values of b, the imaginary part of the shunt impedance.

spectrometer for samples of comparable geometry and dielectric properties.[18,19]

The maximum computed sensitivity for the quartz sample holder in the transmission mode spectrometer occurs for $t=0.015$ mm and $d=0.070$ mm. We have used quartz plates from 0.165 to 0.130 mm thick for our studies because thinner plates are very fragile. However, we plan to try thinner plates in order to try to take advantage of the computed increase in sensitivity by a factor of ≈ 15. We have also examined the sensitivity of sample holders using quartz plates of unequal thickness. This case is interesting since it results in a power imbalance between the side of the resonator that faces the detector and the side facing the source. However, the calculated sensitivity decreased for any small nonsymmetric changes in the quartz plate thicknesses relative to the point of $t=0.015$ mm and $d=0.070$ mm. This result could be anticipated from a lumped circuit analysis,[18,27] for which parameters such as coupling constants enter into the equation for sensitivity as interchangeable pairs. In taking derivatives to maximize sensitivity with respect to these parameters, we thus find they must have equal values. This reasoning does not necessarily hold for a reflection-mode spectrometer.

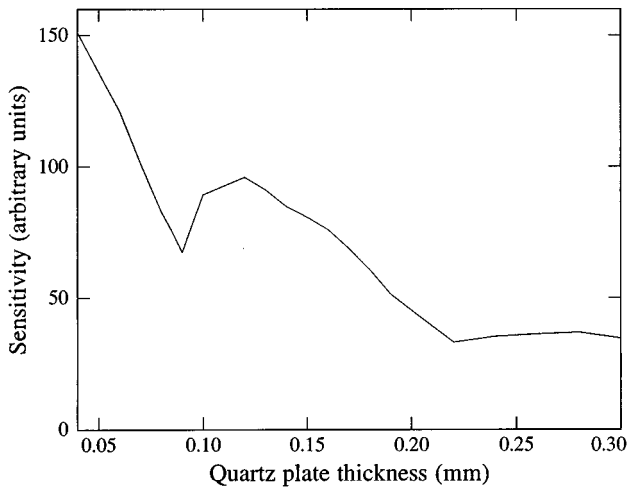

FIG. 8. The calculated sensitivity of the quartz plate sample holder of variable thickness, with a 0.02-mm-thick aqueous sample, for a reflection mode spectrometer, neglecting all other factors that influence spectrometer sensitivity. The quartz plates are of equal thickness and the mirror impedance is $Y=0+i30$.

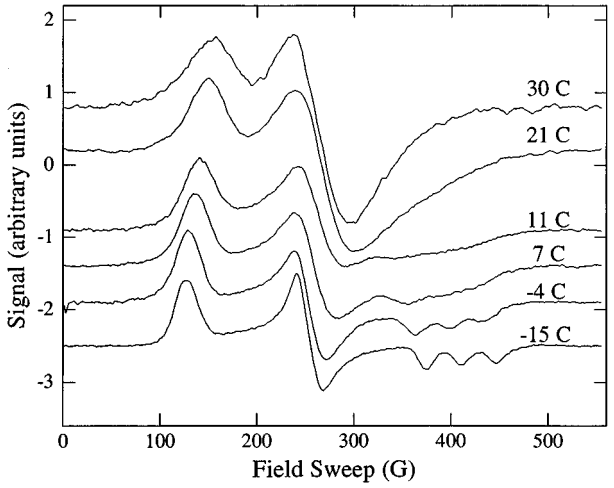

FIG. 9. A series of 250 GHz ESR spectra of DUMTA (Ref. 3) recorded in a 75% glycerol to 25% water mixture at several temperatures.

We now show a few examples of 250 GHz ESR spectra we have obtained using this sample holder in a transmission mode setup. Figure 9 shows a series of ESR spectra of the nitroxide-labeled nucleoside 5-[[(2,2,6,6-tetramethyl-1-oxo-4-piperidyl)amino]methyl]-2′-deoxyuridine (DUMTA),[3] recorded in a 75% glycerol/25% water solution using two flat quartz plates and a third quartz plate with a 10-mm-diam hole bored through as a spacer. Higher sensitivity was achieved for this thicker sample since dielectric losses in the glycerol/water mixture are lower than for pure H_2O. These spectra nicely demonstrate how the enhanced resolution to the g tensor at 250 GHz provides detailed information of the molecular motion of the spin probe. For this case, the nitroxide tumbles more rapidly along its N–O bond, which is roughly parallel to the tether connecting the nitroxide to the thymidine, than perpendicular to it. As a result, the peaks in the line shapes that represent g_{yy} and g_{zz} are averaged together to a greater degree than the peak for g_{xx}. For the case of T4 Lysozyme, an enzyme with a molecular weight of 18 600, labeled with a nitroxide at site 69 and dissolved in a pH-buffered aqueous solution,[6] a sample thicknesses of 0.017 mm yielded an optimum sensitivity as expected from the above analysis. The 250 GHz ESR spectra are shown in Fig. 10. There was ~1 mM of spin label present in an ESR active volume of 0.25 μL. Although the signal-to-noise for one sweep was ~60 due to the 300 G linewidths, 50 sweeps produced ESR spectra with sufficient resolution for a line shape analysis. These line shapes convey information about

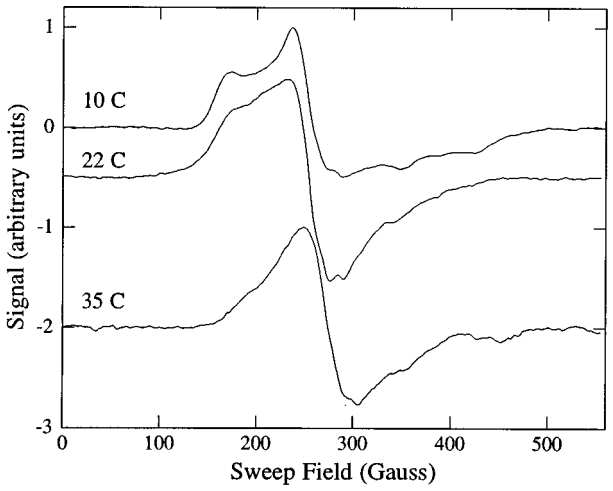

FIG. 10. 250 GHz ESR spectra of T4 Lysozyme, labeled with a nitroxide at site 69 (Ref. 6) recorded in a *p*H-buffered aqueous solution of thicknesses from 0.01 to 0.02 mm at several temperatures.

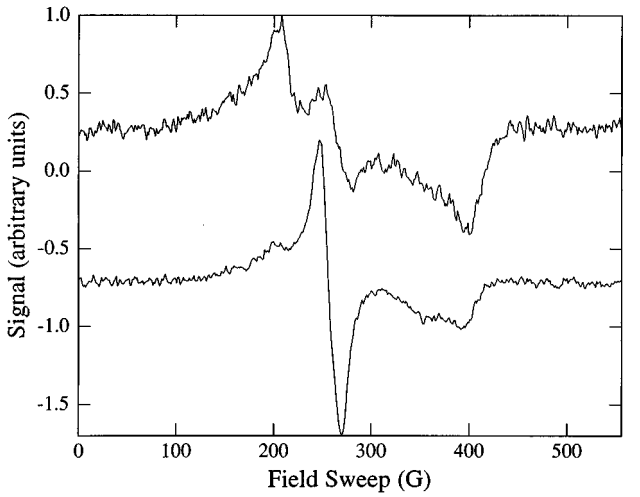

FIG. 11. 250 GHz ESR spectra of DMPC vesicles containing the spin label CSL, hydrated in a 100% relative humidity atmosphere at 23 °C, and recorded at 52 °C (top) and at 60 °C (bottom). The top spectrum is that of a randomly oriented MOMD sample and the bottom one is for a partially aligned sample.

the motion and steric constraints imposed on the nitroxide's motion by the protein.

Figure 11 shows the 250 GHz ESR spectrum of a fully hydrated vesicle solution of 1,2-dimyristoyl-sn-glycero-3-phosphatidylcholine (DMPC) with 3 mole % 3β-doxyl-5α-cholestane (CSL) present as a spin label which orients itself in the hydrocarbon chain layer of the vesicles. In the top spectrum the vesicles are randomly oriented while in the bottom spectrum they are partly aligned so that a greater proportion of the membrane surfaces are normal to the applied static magnetic field. This can be inferred from the change from a microscopically ordered but macroscopically disordered (MOMD) type spectrum[36] (top spectrum) to a spectrum in which the g_{yy} region is preferentially weighted (bottom spectrum). The spectra were recorded at 52 and 60 °C in a sample holder that used PETE as the plate material and had a silicon rubber o-ring seal to prevent evaporation from the sample. (Buna-N o-rings have ESR backgrounds.) Sample holders that use polymers are more flexible than those using quartz, which is an advantage for the preparation of some kinds of model membrane samples. However, we find they also tend to have lower sensitivity possibly because their curved surfaces scatter the FIR radiation.

In summary, a sample geometry design for obtaining high-frequency ESR spectra from aqueous samples has been demonstrated. Optimization of the sample holder was done utilizing quasioptical design techniques. The maximum sensitivity to ESR occurs when the aqueous sample layer is from 0.01 to 0.03 mm thick when held between quartz plates 0.165 mm thick. The highest sensitivity experimentally measured on the 250 GHz ESR spectrometer operating in a transmission mode was 2×10^9 spins/G, on a 0.27 mM aqueous solution of tempamine. It occurred for an aqueous layer thickness of 0.017 mm, corresponding to a sample volume of 0.3 μl and 4×10^{13} spins in the ESR ''active'' region of the FP resonator. The sample holder is easy to construct and is adaptable to a wide range of studies of biological systems at temperatures of relevance.

ACKNOWLEDGMENTS

The authors wish to acknowledge many helpful discussions with Dr. Keith Earle. They also wish to express their gratitude to Professor Albert Bobst and Elizabeth Bobst for providing the DUMTA sample and to Professor Wayne Hubbell and Professor Hassane Mchaourab for providing the spin-labeled T4 Lysozyme samples. This work was supported by NIH Grant Nos. RR07216 and GM25862. JPB was supported by a National Research Service Award No. GM17174.

[1] *EPR and Advanced EPR Studies of Biological Systems*, edited by L. D. Dalton (Chemical Rubber, Boca Raton, FL, 1985).
[2] H. S. Mchaourab, M. A. Lietzow, K. Hideg, and W. L. Hubbell, Biochemistry **35**, 7692 (1996).
[3] R. S. Keyes and A. M. Bobst, Biochemistry **34**, 9265 (1995).
[4] M. Ge, D. E. Budil, and J. H. Freed, Biophys. J. **66**, 1515 (1994); **67**, 2326 (1994).
[5] See, for example, *Spin Labeling: Theory and Applications, Biological Magnetic Resonance*, edited by L. J. Berliner and J. Reuben (Plenum, New York, 1989), Vol. 8.
[6] W. L. Hubbell and C. Altenbach, Curr. Opinion Struct. Biol. **4**, 566 (1994).
[7] D. Budil, K. Earle, and J. H. Freed, J. Phys. Chem. **97**, 1294 (1993).
[8] A. Patkowski, W. Eimer, and Th. Dorfmüller, Biopolymers **30**, 975 (1990).
[9] J. Gibrat and N. Go, Proteins: Structure, Function Genetics **8**, 258 (1990); M. Levitt, C. Sander, and P. S. Stern, J. Mol. Biol. **181**, 423 (1985).
[10] K. A. Earle, J. K. Moscicki, M. Ge, D. E. Budil, and J. H. Freed, Biophys. J. **66**, 1213 (1994).
[11] A. I. Smirnov, T. I. Smirnova, and P. D. Morse II, Biophys. J. **68**, 2350 (1995).
[12] V. I. Krinichnyi, Biochem. Biophys. Methods **23**, 1 (1991).
[13] J. B. Hasted, *Aqueous Dielectrics* (Chapman and Hall, London, 1973), Chap. 2.
[14] J. Barthel, K. Bachhuber, R. Buchner, and H. Hetzenauer, Chem. Phys. Lett. **165**, 369 (1990).
[15] (a) J. B. Hasted, S. K. Husain, F. A. M. Frescura, and J. R. Birch, Chem. Phys. Lett. **118**, 622 (1985); (b) Infrared Phys. **1**, 11 (1987).
[16] M. N. Afsar and J. B. Hasted, J. Opt. Soc. Am. **67**, 902 (1977).
[17] R. E. Collins, *Foundations for Microwave Engineering*, 2nd ed. (McGraw-Hill, New York, 1992), Chaps. 3–5.

[18] K. A. Earle, D. E. Budil, and J. H. Freed, in *Advances in Magnetic and Optical Resonance*, edited by W. S. Warren (Academic, San Diego, 1996), Vol. 19.
[19] K. A. Earle, D. S. Tipikin, and J. H. Freed, Rev. Sci. Instrum. **67**, 2502 (1996).
[20] W. B. Lynch, K. A. Earle, and J. H. Freed, Rev. Sci. Instrum. **59**, 1345 (1988).
[21] J. Lesurf, *Millimeter Wave Optics, Devices and Systems* (Adam Hilger, Bristol, 1990), Chap. 1.
[22] H. Kogelnik and T. Li, Proc. IEEE **5**, 1550 (1966).
[23] Keith Earle, Baker Laboratory of Chemistry, Cornell University (private communication).
[24] P. K. Yu and A. L. Cullen, Proc. R. Soc. London, Ser. A **380**, 49 (1982).
[25] S. Nemoto, Appl. Opt. **27**, 1833 (1988).
[26] J. Arnaud, A. A. M. Saleh, and J. Ruscio, IEEE Trans. Microwave Theory Tech. **MTT-22**, 486 (1974).
[27] G. Feher, Bell System Tech. J. **36**, 449 (1957); see also C. P. Poole, Jr., *Electron Spin Resonance: A Comprehensive Treatise on Experimental Techniques* (Interscience, New York, 1967), Chap. 14.
[28] G. T. McNice and V. E. Deer, IEEE J. Quantum Electron. **12**, 569 (1969).
[29] T. Matsui, K. Araki, and M. Kiyokawa, IEEE Trans. Microwave Theory Tech. MTT **41,** 1710 (1993).
[30] ESCO Products, Inc., 171 Oak Ridge Rod, NJ 07438-0155.
[31] J. R. Birch, J. D. Dromey, and J. Lesurf, Infrared Phys. **21**, 225 (1981).
[32] Dave Wise, Chemistry Department, Cornell University (personal communication).
[33] J. S. Hyde and W. K. Subczynski, in *Biological Magnetic Resonance*, edited by L. J. Berliner and J. Reuben (Plenum, New York, 1989), Vol. 8.
[34] J. S. Hyde and W. K. Subczynski, J. Magn. Reson. **56**, 125 (1984).
[35] M. Sueki, G. A. Rinard, S. S. Eaton, and G. R. Eaton, J. Magn. Reson. A **118**, 173 (1996).
[36] M. Ge and J. H. Freed, Biophys. J. **65**, 2106 (1993).